Journal of Chemical Neuroanatomy 94 (2018) 75–85

Contents lists available at ScienceDirect

Journal of Chemical Neuroanatomy

journal homepage: www.elsevier.com/locate/jchemneu

Pluchea lanceolata protects hippocampal neurons from endothelin-1 induced ischemic injury to ameliorate cognitive deficits

Ravi Mundugaru[a], Senthilkumar Sivanesan[a], Aurel Popa-Wagner[b], Padmaja Udaykumar[c], Ramalingam Kirubagaran[d], Guruprasad KP[e], D.J. Vidyadhara[f,*]

[a] Department of Research and Development, Saveetha University, Chennai, 602 105, India
[b] Department of Neurology, University of Medicine Rostock, Rostock, Germany
[c] Department of Pharmacology, Father Muller Medical College, Mangalore, 575 002, India
[d] Department of Marine Biotechnology, National Institute of Ocean Technology, Chennai, 600100, India
[e] Department of Ageing Research, School of Life Sciences, Manipal University, Manipal, India
[f] Department of Neurophysiology, National Institute of Mental Health and Neuro Sciences, Hosur Road, Bangalore, 560029, India

ARTICLE INFO

Keywords:
Hippocampus
Endothelin-1
Ischemic brain injury
Learning and memory
Dendritic arborization
Glutathione peroxidase

ABSTRACT

Ischemic brain injury is one of the leading causes of death and disability, where lack of disease modifying treatment strategies make us rely on symptomatic relief. Treatment principles from traditional systems of medicine may fill this gap and its validation in modern medicine perspective is important to bring them to mainstream. Here, we evaluated the neuroprotective efficacy of Ayurvedic medicinal herb *Pluchea lanceolata* in treating ischemic hippocampal injury. Focal hippocampal ischemia was modeled in Wistar rats through stereotaxic intrahippocampal injection of endothelin-1 (ET-1). Post-surgery, hydroalcoholic extract of the rhizome of *Pluchea lanceolata* (HAPL) was administered orally, once in a day for 14 consecutive days to ischemic rats. There were two treatment groups based on the HAPL dosage; HAPL200 (200 mg/kg body weight) and HAPL400 (400 mg/kg body weight). Comparisons were made with the ET-1 ischemic rats which received only the vehicle, and the normal surgical control. Ischemic hippocampal injury led to severe cognitive deficits as evaluated by Morris water maze and open field test, along with locomotory dysfunction noted in actophotometer test. HAPL treatment significantly attenuated these behavioural deficits in a dose dependent manner. Loss of pyramidal cells and degenerative phenotype of shrunken hyperdensed soma with pyknotic nuclei in CA1 and CA3 hippocampal neurons in ischemia were reversed after HAPL treatment. We provide first evidence for loss of dendritic architecture in ET-1 induced focal ischemic hippocampal injury using Golgi impregnation, where HAPL could salvage the dendritic branching and intersections. Intriguingly, it enhanced the dentritic arborization beyond what is noted in normal rats. Ability of HAPL to reverse oxidative stress, especially through maintaining glutathione peroxidase levels and lipid peroxidation in ischemic condition evidences that it may exert neuroprotection through its antioxidant properties. Thus, *Pluchea lanceolata* and its constituents provide potential alternative/adjuvant treatment strategy for ischemic hippocampal stroke.

1. Introduction

Hippocampus is involved in learningand memory, which is one of the highly vulnerable areas of the brain to ischemic injury and stroke (Dalley et al., 2004). Stroke is the 2nd most leading causes of death and long term neurological disabilities, especially in elderly population (Donnan et al., 2008). Ischemic stroke results in loss of blood supply to the vital areas of brain followed by a cascade of debilitating events, begins with increased accumulation of excitotoxic neurotransmitters and calcium ions. This in turn causes severe oxidative stress and inflammation, leading to cellular apoptosis and neurodegeneration (Iadecola and Alexander, 2001; Langdon et al., 2010). Lack of

Abbreviations: HAPL, hydro alcoholic extract of *Pluchea Lanceolata*; ET-1, endothelin 1; NE, northeast; SE, southeast; SW, southwest; NW, northwest; MCAO, middle cerebral artery occlusion; ROS, reactive oxygen species; CAT, catalase; GSH-Px, glutathione peroxidase; SOD, superoxide dismutase; TBARS, thio-barbituric acid reactive substances; MDA, malondialdehyde; CNS, central nervous system; H_2O_2, hydrogen peroxide; CA, cresyl violet; CA1, Cornu Ammonis 1; CA3, Cornu Ammonis 3; ANOVA, analysis of variance; SEM, standard error of mean

* Corresponding author. Present address: Departments of Neurology and Neuroscience, Yale University School of Medicine, New Haven, CT, 06519, USA.
E-mail address: vidyadhara.dj@gmail.com (D.J. Vidyadhara).

https://doi.org/10.1016/j.jchemneu.2018.09.002
Received 22 August 2018; Received in revised form 24 September 2018; Accepted 27 September 2018
Available online 29 September 2018
0891-0618/

satisfactory treatment in modern medicine for ischemic stroke is pushing researchers to find cues from traditional systems of medicine like Ayurveda (Lakhotia, 2013).

Pluchea lanceolata (*P. lanceolata*) is a medicinal herb, widely used in Ayurveda for the treatment of arthritis, inflammatory disorders, paralysis, pain of neurological origin, hemiplegia, along with bone and muscle pain (Sharma, 2005; Srivastava and Shanker, 2012). It is one of the important *Rasayana* herb (rejuvenator) used in more than 82 classical formulations for disease management (Srivastava and Shanker, 2012). The extract of this herb have also shown therapeutic potential as immunosuppressant, anti-neoplastic, anti-malarial, anti-oxidant and muscle relaxant, which was also mentioned to have central nervous system stimulant and neuroprotective action (Bhagwat et al., 2010; Jahangir et al., 2005; Jahangir and Sultana, 2006; Mohanty et al., 2013; Srivastava et al., 2014; Srivastava and Shanker, 2012). We have recently demonstrated the neuroprotective functions of hydroalcoholic extract of *P. lanceolata* (HAPL) against aluminum chloride-induced neurotoxicity in mice (Mundugaru et al., 2017). Among triterpenes, pluchine, quercetin, quercetrin, flavonoids and taraxasterol are known bioactive components of *P. lanceolata* (Prasad et al., 1965). The chemical constituents of triterpene have various neuroprotective actions. Both *in vitro* and *in vivo* studies have revealed that the treatment with taraxasterol significantly attenuates the release of pro-inflammatory cytokines such as TNF-α, IFN-γ and IL-6 in lipopolysaccharide induced neuroinflammation (Srivastava et al., 2014). Several of these pharmacological properties appear to be beneficial in cerebral ischemia.

Endothelin-1 (ET-1) is a potent vasoconstrictor. In brain, it is produced predominantly in the endothelium of the cerebral micro-vessels, and also in the neurons and glia (Hynynen and Khalil, 2006). ET-1 acts through G-protein coupled receptor such as ET_A and ET_B (Baba, 1998). The ET_A receptors have high specificity for ET-1 and are expressed in brain vascular cells, whereas ET_B receptors are non-selective and are randomly expressed in neurons and glial cells (Rozyczka et al., 2004). High levels of ET-1 in patients with neurological disorders such as Alzheimer's disease, subarrachnoid hemorrhage, traumatic brain injury and ischemic stroke implicates its role in neuronal damage (Muir et al., 2007). Its ability to bring acute vasoconstriction by acting through ET_A receptors have been widely exploited to model ischemic brain injury (Dai et al., 2017; Driscoll et al., 2008; Hughes et al., 2003; Tsenov et al., 2007). Intrahippocampal injection of ET-1 can cause neuronal excitability and acute seizures, mainly due the ischemic damage (Blomstrand et al., 2004) and aptly recapitulate the neurodegenerative cascades and cell death noted in ischemic hippocampal stroke (Driscoll et al., 2008).

In this study, we have investigated the neuroprotective functions of hydroalcoholic extract of *Pluchea lanceolata* (HAPL) in a rat model of ET-1 induced hippocampal stroke. Cognitive behavioural assessments were done to evaluate hippocampal functions, followed by histological studies focusing CA1 and CA3 hippocampal sub-regions. Neuronal dendritic architecture was also evaluated. We then conducted biochemical assays to delineate the potential target for putative neuroprotective action of *P. lanceolata* in ischemic hippocampal injury.

2. Materials & methods

2.1. Plant material and extract preparation

The rhizome of *P. lanceolata* were procured from Jamnagar, India and authenticated in Pharmacognosy laboratory at SDM Centre for Research in Ayurveda and Allied Sciences, Udupi, Karnataka, India. The voucher specimen no. 15031401-02 was deposited for future reference. The rhizome was shade dried and powdered at SDM Pharmacy, Udupi, Karnataka, India with the help of pulverizer. The hydroalcoholic extract was prepared by soaking 500 g of powdered rhizome of *P. lanceolata* in 2 liters of 50% ethanol and 50% cold distilled water for 24 h, filtered and concentrated by evaporating on water bath till free from water.

2.2. Animals

Male Wistar albino rats of 6–8 months old, weighing 350–400 g each were obtained from animal house affiliated to the Pharmacology and Toxicology laboratory at SDM Centre for Research in Ayurveda and Allied Sciences, Udupi, Karnataka, India. The animals were maintained at standard laboratory conditions such as temperature at 25–27 °C, humidity of 50–55% and natural light and dark cycles (Gopalakrishanan et al., 2016). Animals were fed with commercial pellet diet (Pranav agro Industry, Pune) and water *ad libitum*. Prior to the experimentation, approval was obtained from institutional animal ethical committee (Reference no. SDMCAU/IAEC/PH-01/2014-15), which adheres to National Institute of Health, USA guidelines.

2.3. Animal groups and HAPL administration

The randomly selected Wistar rats were categorized into 4 different groups (n = 6–8/group/experiment). Vehicle group rats underwent sham-surgery and administered with 0.5% carboxylmethyl cellulose (CMC) orally (p.o., 5 ml/kg body weight) and considered as vehicle control. ET-1 group was administered with single intrahippocampal injection of 80 μM ET-1 prepared in 0.1 M phosphate buffer saline (PBS, pH 7.4), followed by the vehicle, 0.5% CMC administered orally for 14 consecutive days. "ET-1 + HAPL200" group was administered with 200 mg/kg body weight of HAPL prepared in 0.5% CMC for 14 consecutive days (p.o, 5 ml/kg body weight) after single intrahippocampal injection of 80μM ET-1. A higher dose of 400 mg/kg body weight of HAPL was administered p.o. in "ET-1 + HAPL400" group for 14 days, after the intrahippocampal injection of ET-1 (Mundugaru et al., 2017).

2.4. surgical procedures to produce ET-1 induced ischemic hippocampal stroke

Ischemic hippocampal stroke was induced by unilateral intrahippocampal injection of ET-1, directly into the right hippocampus of Wistar rats (Fuxe et al., 1997; Hughes et al., 2003; Tsenov et al., 2007). Rats were anesthetized with single intraperitoneal injection of sodium pentobarbitone (45 mg/kg), following which head was shaved and fixed to the stereotaxic apparatus (Stoelting, USA). Using scalpel, a midline incision was made and the connective tissue was removed with the help of dry sterile cotton swab to locate the bregma on the skull. A small drill hole was made in the right side of skull at unilateral coordinates from bregma (anteroposterior: 4.5 mm; mediolateral: 4.0 mm; dorsoventral: 3.5 mm from the skull surface) (Faraji et al., 2014; Sheng et al., 2015). An infusion syringe (23 gauge, Hamilton, USA) (Faraji et al., 2014) was loaded with ET-1 (80 μM in PBS) and mounted in the stereotaxic injector. The needle tip was lowered through the drilled hole targeted for placement directly into the hippocampus. Three microliters of 80 μM ET-1 was infused at a rate of 1 μL per minute and the syringe was left in the place for 3 min after the infusion and slowly removed. The incision was closed with 3.0 nylon suture under aseptic conditions following which rat was placed in a warm and dry recovering area for seven days with free access to soft food and water.

2.5. Behavioural evaluation for hippocampal function

2.5.1. Open field test (exploratory behaviour)

The apparatus consists of square box of 96 x 96 cm dimensions with side walls about 30 cm high as described by Bhattacharya et al. (1997). The floor was divided into 36 equal squares. The rats were kept in a dim light and quiet area during the experiment. Each rat was gently placed in the pre-determined corner of the apparatus an hour after drug administration and allowed to explore the arena for 5 min (Suresh et al., 2017). The following parameters were recorded: the number of rearing, number of fecal pellets expelled, number of squares crossed, duration of immobility (freezing time), and the time of initiation. The open field

test was conducted for all the group of rats on 14th day after hippocampal ischemia.

2.5.2. Actophotometer test (locomotor activity)

Locomotor activity was assessed by using digital actophotometer. The motor activities were recorded for a period of 5 min by means of photocells and counters activated by the movement of rat across the light beam inside the actophotometer chamber (Bansinath et al., 1982). Locomotor assessment was made in all the groups on 14th day after hippocampal ischemia.

2.5.3. Morris water maze test (spatial memory)

Morris water maze is the most widely accepted test for assessment of spatial working memory in laboratory animals (Bromley-Brits et al., 2011; Vorhees and Williams, 2006). The water maze contained a circular water pool with 150 cm diameter and 40 cm height. The water pool was divided into northeast (NE), southeast (SE), southwest (SW) and northwest (NW); equally spaced quadrants along the circumference of the pool. In the NW quadrant, an escape platform (10 cm diameter) was kept, 2 cm below the water surface. Throughout the acquisition trials, this platform was maintained constantly in NW quadrant. The rats were trained to locate this hidden platform. If the rat failed to find the platform within 60 s, it was gently guided to the platform and was allowed to stay there for 15 s and explore the surroundings. Animals had four acquisition trials per day for four consecutive days, starting from day 9th and ending on day 12th post-surgery. To eliminate the quadrant affects, animal was positioned in each quadrant during each trial. Animals that failed to reach the platform in 60 s on the 4th trial day were excluded from the study (1, 2, 1 and 0 number of rats from Vehicle, ET-1, HAPL200 and HAPL400, respectively). On probe test day (day 13th), 24 h after the last training, acquisition test was performed and time taken to reach the hidden platform was noted as escape latency. In addition, the retention memory was tested on 14th day. Here, escape platform was removed and the animals were allowed to swim for 60 s before the end of session. Latency to find the northwest target quadrant (NW latency) and time spent in target quadrant (NW) which had previously contained the hidden platform was noted (Bromley-Brits et al., 2011). Retention trials, mainly the time spent in the target quadrant indicates the degree of memory consolidation taken place after learning.

2.6. Histopathology of hippocampal region of the brain

2.6.1. Cresyl violet staining to evaluate CA1 and CA3 neuronal cells of the hippocampus

At the end of behavioural studies, the rats were euthanized by sodium pentobarbitone (100 mg/kg body weight, i.p.). The brains were carefully dissected out, fixed in 10% formalin and processed for paraffin embedding. Six brain samples from each group were used. 8 µm coronal sections were obtained using rotary microtome (Leica RM 2155, Germany), out of which ten sections per animal were used for histopathalogical study. The sections were stained with cresyl violet using standard procedure (Jyothi et al., 2015). All slides were then evaluated under light microscope (ZEISS Axio lab A1, Germany).

2.6.2. Quantification of surviving neurons of CA1 & CA3 region

Quantitative analysis of cresyl violet (CV) stained cells was carried out by a person who was blind to the group of animals. The neurons in the control group and the surviving neurons from all the treatment groups in the CA1 and CA3 regions were quantified in 1 mm^2 area focused using Axio cam ERc 5s (ZEISS, Germany) software. The total number of normal neuronal cell bodies (with normal cell membrane, nucleus with even staining) were assessed. Sections were also evaluated for presence of darkly stained, irregular and shrunken pyramidal cells with pyknotic nuclei.

2.6.3. Golgi cox staining to analyze dendritic arborization

Gogli cox staining method is the gold standard method to study the neuronal dendritic arborization. After the experimental period, the animals were euthanized with sodium pentobarbitone (100 mg kg body weight, i.p. injection). The brains were dissected out carefully and impregnated in modified Golgi–Cox stain for 2 weeks and processed as reported earlier by Narayanan et al. (2014). Briefly, coronal sections of 170 µm were obtained using a vibratome [Leica VT1000 S, Germany] and collected over gelatin coated slides. They were immediately transferred to slotted cassettes submerged in a Petri dish containing distilled water, following which slides were drained off the excess water using blotting paper. Sections were then submerged in 6% sodium carbonate solution for 20 min in dark condition. Following wash in distilled water, sections were dehydrated in increasing concentration gradients of alcohol (70%, 80%, 90% and 100%) for 5 min each and finally in xylene for 20 min. Slides with the sections were then mounted using Dibutylphthalate Polystyrene Xylene (DPX) and cover slipped. The slides were air dried and subjected to analysis.

2.6.4. Quantification of dendritic arborization using camera lucida

Hippocampal pyramidal neurons from CA1 and CA3 regions of both hemispheres (10 per animal, 60 in each group) were viewed under 400× magnification using a camera lucida (LABKRON, India) fixed to a monocular microscope. Neurons selected for camera lucida tracing were based on the following selection criteria.

a A neuron must confine to CA1 and CA3 regions of the hippocampus.
b Neurons selected must be darkly stained and the entire dendritic profile should be identifiable.
c No truncation of any branch should be present within 100 µm radius from soma.
d Neurons selected must be comparatively isolated from neighboring neurons.

Apical and basal dendritic branching points and dendritic intersection of CA1 and CA3 pyramidal neurons were quantified by transparent grid with equidistant concentric circle (20 µm) centered over soma. Both branching point and intersections were counted up to a distance of 100 µm from the centre point of soma (Sholl, 1953).

2.7. Biochemical evaluation

2.7.1. Preparation of brain tissue homogenates for biochemical estimation

Brains from all the groups were excised for hippocampus and cleaned with ice cold saline and stored at −20 °C (Vidyadhara et al., 2016, 2017). Shortly before conducting the biochemical estimation, tissues were thawed and homogenized in 0.1 M PBS of pH 7.4, centrifuged at 4 °C and the supernatant collected was subjected to assessment of various biochemical parameters. Excess supernatant of the brain tissue homogenate was stored at −20 °C for further use.

2.7.2. Determination of catalase activity

Hippocampal tissue homogenate (1 mL) was mixed with 5 mL of phosphate buffer (pH 7.4) and 4 mL of 0.2 M H_2O_2 prepared in phosphate buffer. Exactly 180 s after adding H_2O_2, a set of 1 mL reaction mixture from the above was mixed with 2 mL dichromate acetic acid. It was kept in boiling water bath for 10 min, following which all the tubes were cooled under running tap water and spectrophotometric assessment (Systronics 2201, India) was done at 570 nm against reagent blank. Catalase activity in the tissue was expressed as micromoles of H_2O_2 consumed/mg protein/min (Sinha, 1972).

2.7.3. Determination of lipid peroxidation

Lipid peroxidation activity was determined by measuring the content of the thio-barbituric acid reactive substances (TBARS) using UV-Visible double beam spectrophotometer (Systronics 2201, India). The

level of lipid peroxidation was expressed as milli moles of malondialdehyde (MDA) formed/g of wet tissue (Ohkawa et al., 1979).

2.7.4. Determination of glutathione peroxidase

Glutathione peroxidase estimation was based on standard earlier protocol (Rotruck et al., 1973). Briefly, the tissue homogenate (0.2 mL) was added to the test tube containing 0.2 mL of Ethylenediaminetetraacetic acid (EDTA), sodium azide, reduced glutathione, H_2O_2 and 0.4 mL of phosphate buffer (pH 7.4), mixed well and incubated at 37 °C for 10 min. The reaction was arrested by adding 0.5 ml of Trichloroacetic acid (TCA) and centrifuged. The supernatant (0.5 mL) was pipetted into a test tube containing 4 mL of disodium phosphate and 0.5 mL of 5,5-dithio-bis-2-nitrobenzoic acid (DTNB). The colour developed was read at 420 nm (Systronics spectrophotometer 2201, India) immediately and the standards were also treated in a similar manner. The levels of glutathione peroxidase activity were expressed as μM glutathione utilized per mg protein per minute at 37 °C.

2.8. Statistical analysis

The data was analyzed using one-way ANOVA followed by Tukey's post hoc test. For Golgi studies to evaluate dendritic arborization, two-way ANOVA was performed using GraphPad Prism version 6.01 (GraphPad Software, Inc., USA). The values are expressed as mean ± SEM and a p-value lower than 0.05 was considered significant.

3. Results

3.1. Higher dose of HAPL drug ameliorated locomotor defects after hippocampal stroke

The intrahippocampal injection of ET-1 caused a very significant reduction in total locomotor activity as compared to vehicle control (Fig. 1A, ET-1 v/s Vehicle, ****$p < 0.0001$). The locomotion activity was restored in a dose-dependent fashion, with the higher dose of HAPL showing significant recovery when compared to the ischemic hippocampal injury group (Fig. 1A, ET-1 + HAPL400 v/s ET-1, $^{\#}p < 0.05$).

3.2. Ischemic injury-induced deficits in the open field exploratory behaviours were ameliorated after HAPL treatment

The intrahippocampal injection of ET-1 caused significant reduction in the total number of squares crossed (Fig. 1B, ET-1 v/s Vehicle, ****$p < 0.0001$) and loss of rearing behaviour in the open field (Fig. 1E, ET-1 v/s Vehicle, *$p < 0.05$). At the same time, the number of fecal pellet expelled was significantly increased as compared to vehicle control (Fig. 1B, ET-1 v/s Vehicle, ****$p < 0.0001$). Though grooming behaviour was found to be effected by the ET-1 treatment, it was not significant (Fig. 1D, ET-1 v/s Vehicle). Treatment with both 200 mg and 400 mg/kg body weight of HAPL significantly improved the open field exploratory behaviour (Fig. 1B, ET-1, $^{\$\$}p < 0.01$ v/s ET-1 + HAPL200, $^{\#\#}p < 0.01$ v/s ET-1 + HAPL400) and the number of fecal pellet expulsion (Fig. 1C, ET-1, $^{\$}p < 0.05$ v/s ET-1 + HAPL200, $^{\#}p < 0.01$ v/s ET-1 + HAPL400). Improved recovery of the grooming behaviour was noted only in high dose HAPL400 group (Fig. 1D, ET-1 v/s ET-1 + HAPL400, $^{\#}p < 0.05$), whereas recovery of rearing behaviour was not significant (Fig. 1E).

3.3. HAPL drug treatment attenuated ischemic stroke induced learning and memory deficits in Morris water maze

The ET-1 group of rats showed significant increase in the escape latency (Fig. 1F, ET-1 v/s Vehicle, ***$p < 0.001$), NW latency (Fig. 1G, ET-1 v/s Vehicle, **$p < 0.01$) and a decrease in the time spent in the target quadrant (Fig. 1H, ET-1 v/s Vehicle, **$p < 0.01$) as compared to

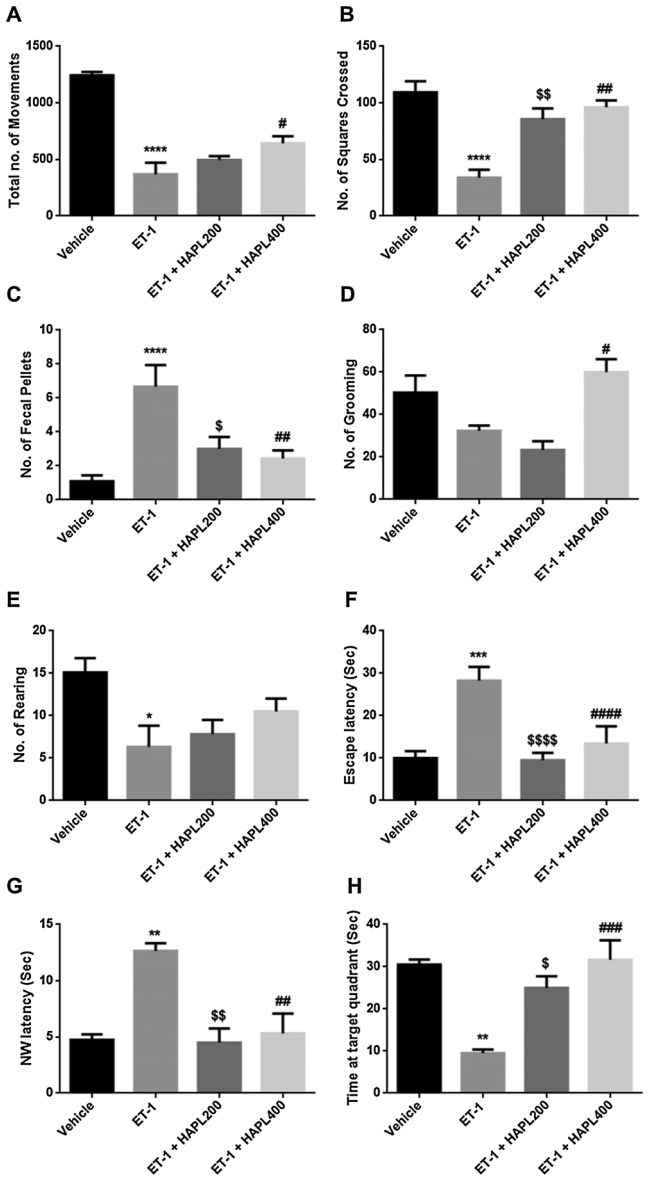

Fig. 1. HAPL treatment attenuated ET-1 mediated ischemic hippocampal injury induced learning and memory deficits. (A) Note reduced number of movements in ET-1 groups (ET-1 v/s Vehicle ****$p < 0.0001$), which was restored in HAPL400 treatment (Fig. 1A, ET-1 + HAPL400 v/s ET-1, $^{\#}p < 0.05$). (B) Note a recovery in total number of squares crossed in open filed post HAPL treatment (ET-1 v/s Vehicle, ****$p < 0.0001$, ET-1, $^{\$\$}p < 0.01$ v/s ET-1 + HAPL200, $^{\#\#}p < 0.01$ v/s ET-1 + HAPL400). (C) Number of fecal pellets expelled in open field increased after ET-1 injection (v/s Vehicle, ****$p < 0.0001$), but attenuated after HAPL treatment ($^{\$}p < 0.05$ v/s ET-1 + HAPL200, $^{\#}p < 0.01$ v/s ET-1 + HAPL400). (D) Grooming behavior abnormality was reversed after HAPL treatment (Fig. 1D, ET-1 v/s Vehicle; ET-1 v/s ET-1 + HAPL400, $^{\#}p < 0.05$). (E) Number of rearing decreased significantly, where HAPL treatment brought only marginal recovery (Fig. 1E, ET-1 v/s Vehicle, *$p < 0.05$). (F) Note significant increase in escape latency in Morris water maze in ET-1 group (ET-1 v/s Vehicle, ***$p < 0.001$), which was reversed after HAPL treatment (ET-1, $^{\$\$\$\$}p < 0.0001$ v/s ET-1 + HAPL200, $^{\#\#\#\#}p < 0.0001$ v/s ET-1 + HAPL400). (G) Latency to reach northwest (NW) quadrant in water maze was recovered in HAPL groups (ET-1 v/s Vehicle, **$p < 0.01$; ET-1, $^{\$\$}p < 0.01$ v/s ET-1 + HAPL200, $^{\#\#}p < 0.01$ v/s ET-1 + HAPL400). (H) Time spent at target quadrant was also recovered after HAPL treatment (ET-1 v/s Vehicle, **$p < 0.01$; ET-1, $^{\$}p < 0.05$ v/s ET-1 + HAPL200, $^{\#\#\#}p < 0.001$ v/s ET-1 + HAPL400). (For Morris Water Maze, 'n' is 7, 6, 7 and 8 number of rats from Vehicle, ET-1, HAPL200 and HAPL400, respectively).

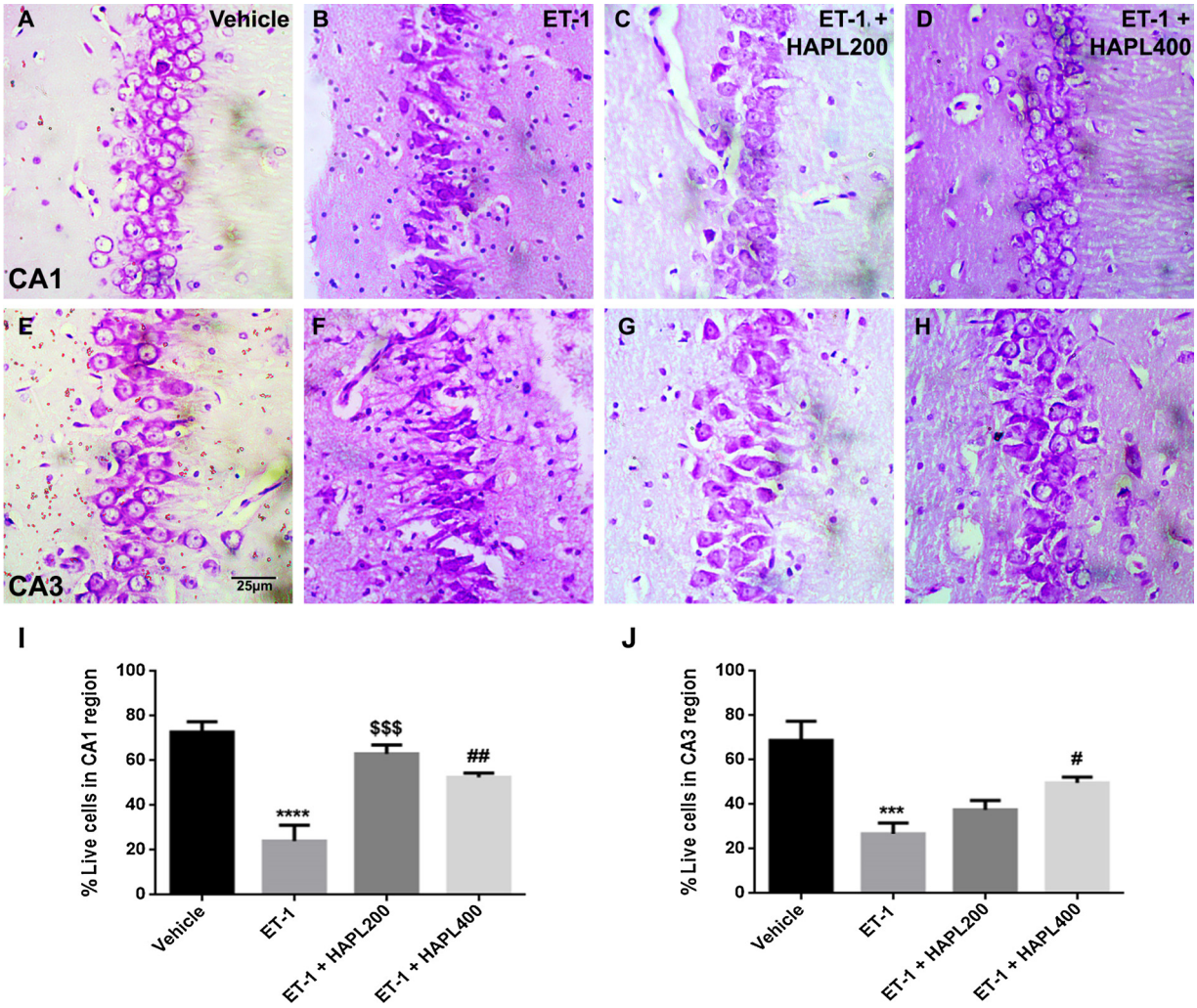

Fig. 2. Pyramidal cells of the CA1 and CA3 regions survived ET-1-induced ischemic injury in the HAPL treatment groups. Representative photomicrographs of CV stained CA1 and CA3 hippocampal pyramidal cells across different treatment groups (A–H). Note compactly arranged healthy pyramidal cells in CA1 (A) and CA3 (E) hippocampal sub-regions of Vehicle group. (B) and (F), Note shrunken hyperdensed cells with pyknotic nuclei in ET-1 group. Note recovery in intactness of pyramidal cell layer with normal neuronal morphology after HAPL treatment, both in the CA1 and CA3 subdivisions of the hippocampus (compare C & D with B, and G & H with F). Note significant loss of cells after ET-1 injection in CA1 (I) and CA3 (J) subregions (CA1, I, ET-1 v/s Vehicle, $^{****}p < 0.0001$; CA3, J, ET-1 v/s Vehicle, $^{***}p < 0.001$). Significant recovery in percentage live cells was noted after HAPL treatment at CA1 (I, ET-1, $^{\$\$\$}p < 0.001$ v/s ET-1 + HAPL200, $^{\#\#}p < 0.01$ v/s ET-1 + HAPL400), where only higher HAPL dosage revealed significance at CA3 (J, $^{\#}p < 0.05$, ET-1 v/s ET-1 + HAPL400). Scale bar: 25 μm.

vehicle control in Morris water maze. Both the doses of HAPL treatment in ischemic injury showed significantly preserved learning and memory as noted by decrease in escape latency (Fig. 1F, ET-1, $^{\$\$\$\$}p < 0.0001$ v/s ET-1 + HAPL200, $^{\#\#\#\#}p < 0.0001$ v/s ET-1 + HAPL400), NW latency (Fig. 1G, ET-1, $^{\$\$}p < 0.01$ v/s ET-1 + HAPL200, $^{\#\#}p < 0.01$ v/s ET-1 + HAPL400) and increase in total time spent in the target quadrants (Fig. 1H, ET-1, $^{\$}p < 0.05$ v/s ET-1 + HAPL200, $^{\#\#\#}p < 0.001$ v/s ET-1 + HAPL400), which were comparable to control rats.

3.4. Pyramidal cells in the CA1 and CA3 regions were protected from ET-1-induced ischemic injury in HAPL treatment groups

Microscopic qualitative examination of the CA1 and CA3 regions of hippocampus in the control group revealed compactly arranged healthy pyramidal cells with nucleus, and intact cell membrane (Fig. 2A and E). The ET-1 group showed darkly stained, irregular shrunken pyramidal cells within the narrow cell layer with ectopic cells and pyknotic nuclei (Fig. 2B and F). The intactness of the pyramidal cell layer was maintained and overall recovery in neuronal morphology was evident after the HAPL treatment, both in the CA1 and CA3 subdivisions of the hippocampus with ET-1 injection (Fig. 2, compare C & D with B, and G & H with F). Quantification for cell number revealed that the ET-1 injection into the hippocampal area significantly reduced the percentage survival of pyramidal neurons in both CA1 and CA3 regions as compared to vehicle control (Fig. 2, CA1, compare B with A, I, ET-1 v/s Vehicle, $^{****}p < 0.0001$; CA3, compare F with E, J, ET-1 v/s Vehicle, $^{***}p < 0.001$). Both 200 and 400 mg/kg body weight of HAPL significantly attenuated the ET-1-induced neuronal loss in the hippocampal CA1 region (Fig. 2, compare C & D with B, I, ET-1, $^{\$\$\$}p < 0.001$ v/s ET-1 + HAPL200, $^{\#\#}p < 0.01$ v/s ET-1 + HAPL400). The percentage survival of cells in the CA3 region in the HAPL400 group was significantly improved as compared to the ET-1 group, but not in the HAPL200 group (Fig. 2, compare H with F, J, $^{\#}p < 0.05$, ET-1 v/s ET-1 + HAPL400).

3.5. Ischemic injury-induced loss of dendritic branching in the CA1 neurons was diminished by the HAPL treatment

Gogli cox staining for dendritic arborization revealed a significant decrease in the mean number of apical dendritic branching points at 20–40, 40–60, 60–80 and 80–100 μm concentric circles of camera

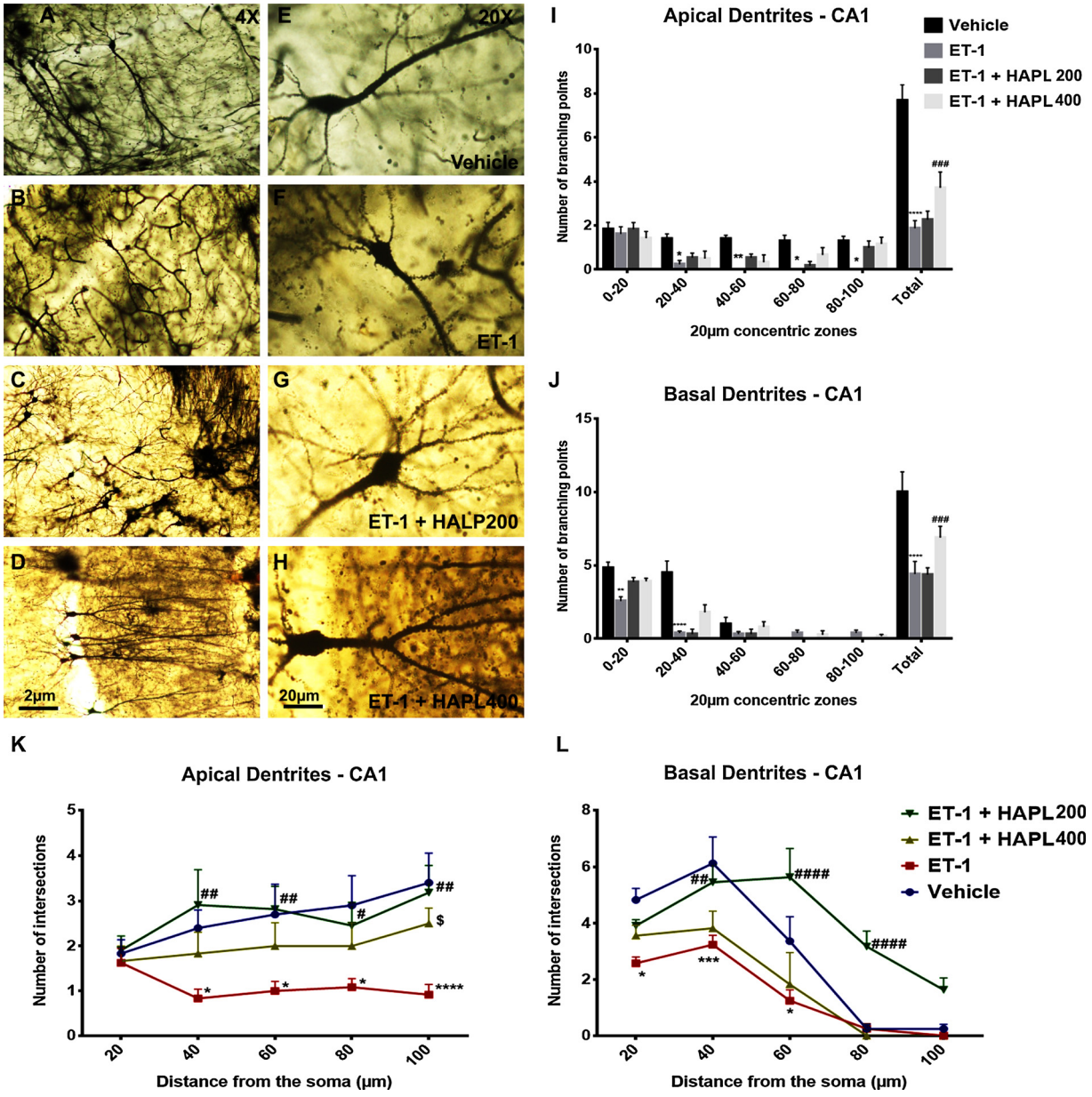

Fig. 3. HAPL treatment preserved dendritic architecture of CA1 hippocampal neurons in ischemic conditions: Representative photomicrographs of Golgi-stained CA-1 hippocampal pyramidal cells at low (10X) and high magnification (40X), in the vehicle (A & E), ET-1 (B & C), ET-1 + HAPL200 (C & G) and ET-1 + HAPL400 (D & H) groups. Note a significant decrease in the number of apical dendritic branching points in the ischemic ET-1 group (I, ET-1 v/s Vehicle, 20–40 *$p < 0.05$, 40–60 **$p < 0.01$, 60–80 *$p < 0.05$, 80–100 *$p < 0.05$, Total ****$p < 0.0001$). Note a significant recovery in total dendritic branching points after high dose HAPL treatment (I, Total, ET-1 v/s ET-1 + HAPL400, $^{###}p < 0.001$). Note a significant loss of basal dendritic branching of CA1 pyramidal cells at different concentric zones in the ET-1 group (J, ET-1 v/s Vehicle, 0–20 **$p < 0.01$, 20–40 **** < 0.0001, Total, ****$p < 0.0001$). Note a significant recovery in HAPL400 group (J, ET-1 v/s HAPL400, $^{###}p < 0.001$). Note a significant reduction in number of apical dendritic intersections of CA1 neurons in ET-1 group (K, ET-1 v/s Vehicle, 40 μm, 60 μm, 80 μm, *$p < 0.05$; 100, ****$p < 0.0001$). Higher HAPL dose significantly preserved these intersections (4 K, ET-1 v/s ET-1 + HAPL400, 40 μm, 60 μm, 100 μm, $^{##}p < 0.01$; 80 μm, $^{#}p < 0.05$), where lower dose was able to preserve those at 100 μm distance away from the soma (K, ET-1 v/s ET-1 + HALP200, 100, $^{$}p < 0.05$). Note a reduction in basal dendritic intersection after ET-1 treatment (L, ET-1 v/s Vehicle, CA1, 20 and 60 μm, *$p < 0.05$; 40, ***$p < 0.001$), which was attenuated significantly after HAPL400 treatment (L, ET-1 v/s ET-1 + HAPL400, 40, $^{##}p < 0.01$, 60 and 80 μm, $^{####}p < 0.0001$). Scale bar: low magnification, 2 μm; high magnification, 20 μm.

lucida in the surviving CA1 neurons of ischemic ET-1 group (Fig. 2, Compare A & E with B & F, I, ET-1 v/s Vehicle, 20–40 *$p < 0.05$, 40–60 **$p < 0.01$, 60–80 *$p < 0.05$, 80–100 *$p < 0.05$). This decrease in branching points at individual concentric zones reflected as the highly significant loss of total apical dendritic branching in the ischemic injury groups (Fig. 3I, Total, ET-1 v/s Vehicle, ****$p < 0.0001$). Although the 400 mg of HAPL treatment revealed only a trend towards recovery in apical dendritic branching in individual concentric zones, a significant rescue was noted when the total dendritic branching points were evaluated (Fig. 3I, Total, ET-1 v/s ET-1 + HAPL high, $^{###}p < 0.001$). In contrast, 200 mg of HAPL treatment was not able to rescue the dendritic branching (Fig. 3I, ET-1 v/s HAPL200).

Basal dendritic branching was negligible at 60–80 μm and 80–100 μm concentric zones in the CA1 subdivision of the control rats (Fig. 3J, Vehicle, 60–80 and 80–100). Unlike apical dendritic branching, basal dendritic branching in the CA1 region were lost even at 0–20 μm concentric zones following the ischemic hippocampal

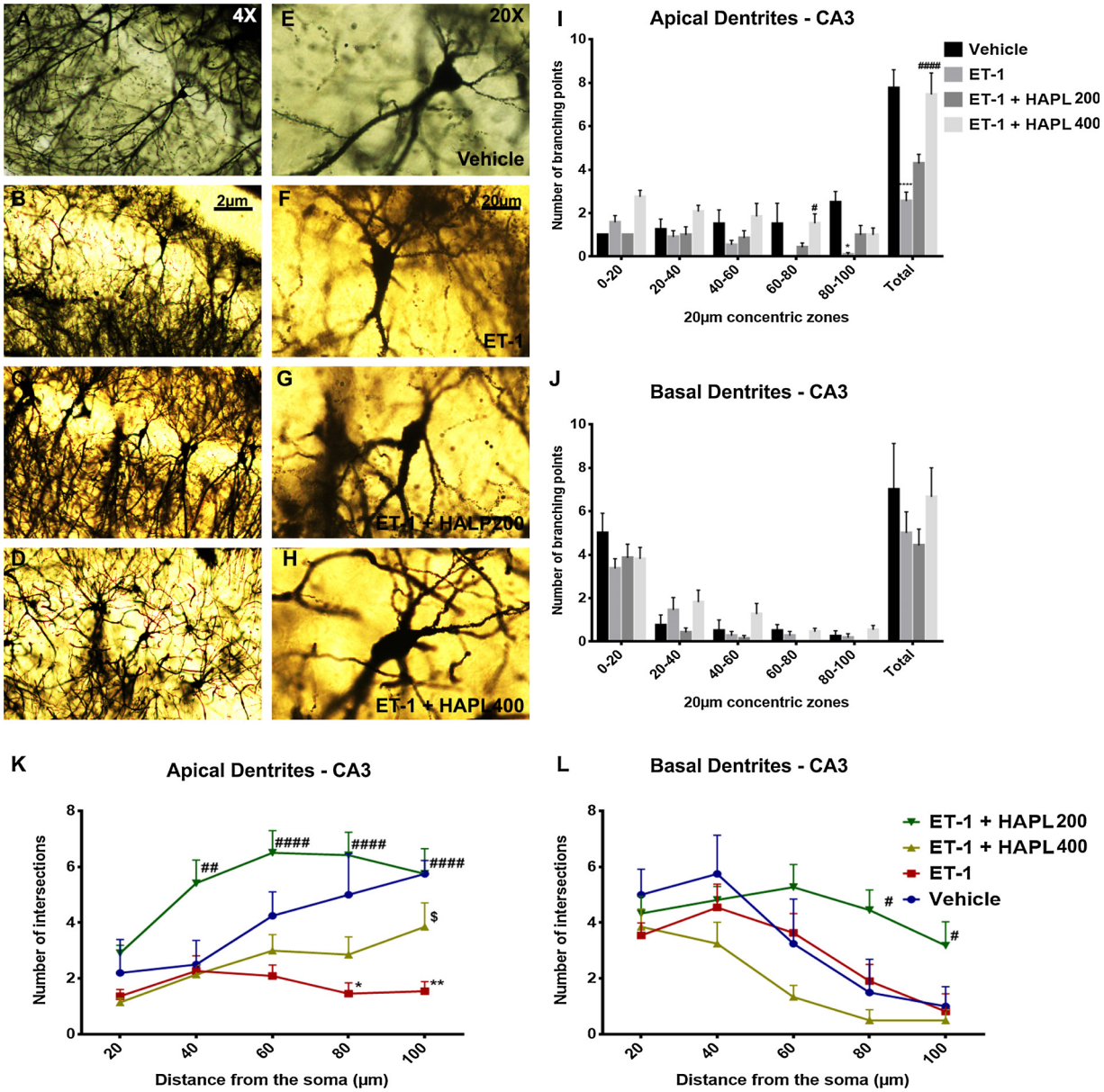

Fig. 4. Loss of dendritic arborization in CA3 hippocampal neurons in ischemic conditions was attenuated after HAPL treatment. Representative photomicrographs of Golgi-stained CA3 hippocampal neurons at low (10X) and high magnification (40X), in the vehicle (A & E), ET-1 (B & C), ET-1 + HAPL200 (C & G) and ET-1 + HAPL400 (D & H) groups. Note a trend in apical dendritic branching loss in the CA3 neurons of ET-1 group at all the concentric zones, with a significance at 80–100 µm, leading to cumulative highly significant loss (I, Vehicle v/s ET-1, 80–100 µm $^{*}p < 0.05$, Total $^{****}p < 0.0001$). Note a significant recovery in HAPL400 group (I, ET-1 v/s ET-1 + HAPL400, 60–80 µm $^{\#}p < 0.05$, Total $^{\#\#\#\#}p < 0.0001$). Basal dendritic branching in the ET-1 group was not effected across treatment groups (J). Note significant loss of CA3 neuronal apical dendritic intersection in ET-1 group (K, Vehicle v/s ET-1, 80 $^{*}p < 0.05$, 100 $^{**}p < 0.01$). A significant recovery was noted only at 100 µm in HAPL200 (K, ET-1 v/s ET-1 + HAPL200, 100 $^{\$}p < 0.05$), whereas, HAPL400 revealed a highly significant increase in apical dendritic intersections at all the distances (K, ET-1 v/s ET-1 + HAPL400, 40 $^{\#\#}p < 0.01$, 60, 80 and 100 µm, $^{\#\#\#\#}p < 0.0001$). Note no effect of ET-1 on basal dendritic intersections of CA3 pyramidal neurons (L, ET-1 v/s Vehicle). Interestingly, HAPL400 significantly enhanced the number of dendritic intersections at 80 and 100 µm when compared to ET-1 and vehicle control (L, ET-1 v/s ET-1 + HAPL400, 80 and 100, $^{\#}p < 0.05$). Scale bar: low magnification, 2 µm; high magnification, 20 µm.

injury, which was also noted for the 20–40 µm concentric zones (Fig. 3J, ET-1 v/s Vehicle, 0–20 $^{**}p < 0.01$, 20–40 $^{****}p < 0.0001$). Though other concentric zones did not reveal significant differences in the loss of branching points, a highly significant reduction in overall number of branching points was noted in the ET-1 group (Fig. 3J, ET-1 v/s Vehicle, Total, $^{****}p < 0.0001$). Concurrently, though maintenance of basal dendritic branching was observed after the HAPL treatment in 0–20 µm and 20–40 µm concentric zones, significance was noted only in the cumulative total number of dendritic branching, where 400 mg/kg body weight of HAPL treatment was able to significantly preserve the branching after the ischemic hippocampal injury (Fig. 3J, ET-1 v/s HAPL high, $^{\#\#\#}p < 0.001$). The lower dose of HAPL did not help in dendritic branching rescue (Fig. 4J, ET-1 v/s HAPL low).

3.6. Dendritic intersection loss in CA1 neurons following hippocampal ischemia was ameliorated at a higher dose HAPL drug

At 20 µm distance away from soma, apical dendritic intersections of CA1 neurons were comparable across all the groups (Fig. 3K, 20 µm). At

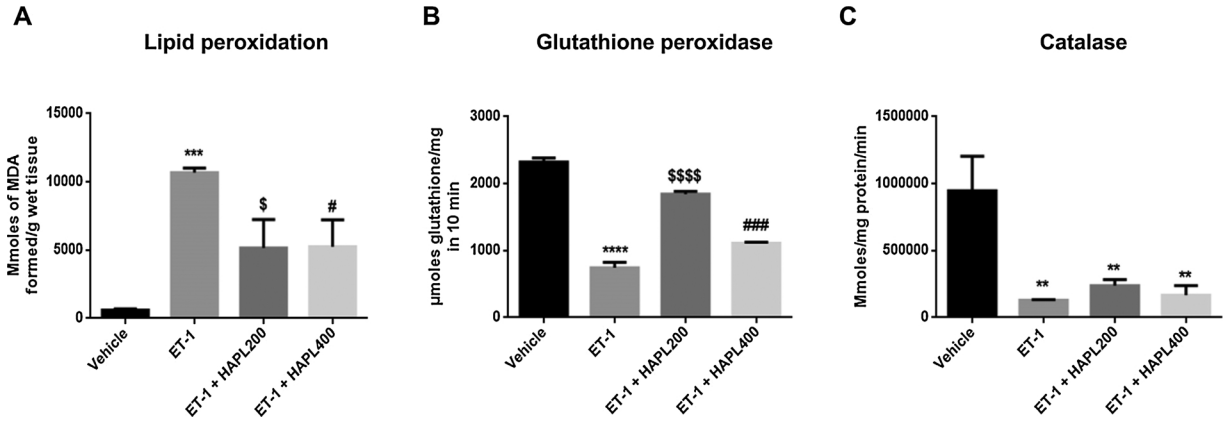

Fig. 5. ET-1 mediated hippocampal oxidative stress was attenuated by the HAPL treatment. (A) Note significant lipid peroxidation in ET-1 groups (ET-1 v/s Vehicle, ***p < 0.01), that was relatively attenuated after HAPL treatment (ET-1, $p < 0.05 v/s ET-1 + HAPL200, #p < 0.01 v/s ET-1 + HAPL400). (B) Glutathione peroxidase level was significantly downregulated after ischemia (ET-1 v/s Vehicle, ****p < 0.0001), which was recovered with HAPL treatment (ET-1, $$$$p < 0.0001 v/s ET-1 + HAPL200, ###p < 0.001 v/s ET-1 + HAPL400). (C) Note a significant reduction in catalase activity (ET-1 v/s Vehicle, **p < 0.01), which was not rescued after HAPL treatment.

40–100 µm away from the soma, number of intersections were significantly reduced in the ischemic injury group, where at 100 µm, a highly significant loss of dendritic intersections was noted (Fig. 3K, ET-1 v/s Vehicle, 40 µm, 60 µm, 80 µm, *p < 0.05; 100, ****p < 0.0001). A higher dose of HAPL significantly reduced the loss of apical dendritic intersections at all levels (Fig. 3K, ET-1 v/s ET-1 + HAPL400, 40 µm, 60 µm, 100 µm, ##p < 0.01; 80 µm, #p < 0.05), whereas at lower dose significant neuroprotection was seen only at 100 µm distance away from the soma (Fig. 3K, ET-1 v/s ET-1 + HALP low, 100, $p < 0.05).

In concurrent with CA1 dendritic branching, no basal dendritic intersections were noted at 80 and 100 µm distance away from the soma in control rats (Fig. 3L, Vehicle, 80 and 100 µm). Basal dendritic intersections were reduced in number after the ischemic hippocampal injury even at 20 µm, which was also evident at 40 µm and 60 µm away from the soma (Fig. 3L, ET-1 v/s Vehicle, CA1, 20 and 60 µm, *p < 0.05; 40, ***p < 0.001). 400 mg of HAPL significantly restored the extent of dendritic intersections at 40, 60 & 80 µm distance away from soma when compared to the ET-1 treatment alone (Fig. 3L, ET-1 v/s ET-1 + HAPL400, 40, ##p < 0.01, 60 and 80 µm, ####p < 0.0001). Interestingly, at 60 and 80 µm away from soma, the higher HAPL treatment after ischemic injury revealed a higher number of dendritic intersections even better than the vehicle control (Fig. 3L, Vehicle v/s ET-1 + HAPL400). 200 mg/kg body weight of HAPL did not have any significant affect in restoring basal dendritic intersections in the CA1 region.

3.7. Loss of apical dendritic branching at CA3 was reversed after HAPL treatment

Golgi staining revealed loss of apical dendritic branching in the CA3 region of ET-1 injected hippocampus, at all the concentric zones of camera lucida, where a significant difference was noted at 80–100 µm concentric zone, leading to cumulative highly significant loss in the total number of dendrites (Fig. 4I, Vehicle v/s ET-1, 80–100 µm *p < 0.05, Total ****p < 0.0001). The low dose of HAPL did not reveal any beneficial effect, whereas treatment with the high dose of HAPL showed rescue of dendritic branching, which was significant at 60–80 µm concentric zones, and also in terms of total dendritic branching (Fig. 4I, ET-1 v/s ET-1 + HAPL400, 60–80 µm #p < 0.05, Total ####p < 0.0001). Interestingly, loss in the number of basal dendritic branching in the CA3 neurons was non-significant in ET-1 group, so as the recovery with HAPL treatment (Fig. 4J).

3.8. HAPL treatment restored ischemia-induced CA3 apical dendritic intersection loss

The numbers of apical dendritic intersections at 20 µm away from soma in the CA3 pyramidal neurons were comparable across all the groups, indicating no effect of either ET-1 injections or HAPL treatment (Fig. 4K and L, 20 µm). At 60 µm, the ET-1 treatment group revealed considerable loss of apical dendritic intersections, which was significant at 80 and 100 µm (Fig. 4K, Vehicle v/s ET-1, 80 *p < 0.05, 100 **p < 0.01). The 200 mg of HAPL treatment showed significant recovery in apical dendritic intersections only at 100 µm (Fig. 4K, ET-1 v/s ET-1 + HAPL200, 100 $p < 0.05). Whereas, the 400 mg/kg body weight of HAPL revealed a highly significant increase in apical dendritic intersections than that was noted in ET-1 treatment group at all the distances from soma (Fig. 4K, ET-1 v/s ET-1 + HAPL400, 40 ##p < 0.01, 60, 80 and 100 µm, ####p < 0.0001). Intriguingly, this increase in the number of dendritic intersections with high dose of HAPL treatment was also observed when compared to vehicle control (Fig. 4K, Vehicle v/s ET-1 + HAPL400, 40, 60 and 80 µm).

ET-1 failed to induce any changes in number of basal dendritic intersections of CA3 pyramidal neurons as seen in vehicle control group (Fig. 4L, ET-1 v/s Vehicle). Interestingly, higher dose of HAPL was associated with a higher number of dendritic intersections at 80 and 100 µm concentric zones as compared with ET-1 and vehicle control (Fig. 4L, ET-1 v/s ET-1 + HAPL400, 80 and 100, #p < 0.05).

3.9. Ischemic hippocampal injury mediated oxidative stress was attenuated by the HAPL drug treatment

Lipid peroxidation in the ET-1 group was significantly increased after ischemic hippocampal injury (Fig. 5A, ET-1 v/s Vehicle, ***p < 0.001), thereby indicating oxidative degradation of lipids. Both 200 and 400 mg kg body weight of HAPL treatment led to attenuation of oxidative stress response in ischemic rats, as noted by the significant reduction in lipid peroxidation levels (Fig. 5A, ET-1, $p < 0.05 v/s ET-1 + HAPL200, #p < 0.01 v/s ET-1 + HAPL400). ET-1 administration also led a significant downregulation of antioxidant enzyme activities such as glutathione peroxidase (Fig. 5B, ET-1 v/s Vehicle, ****p < 0.0001) and catalase (Fig. 5C, ET-1 v/s Vehicle, **p < 0.01). HAPL drug administration, both at 200 and 400 mg doses revealed a highly significant preservation of hippocampal glutathione peroxidase levels in ischemic conditions (Fig. 5B, ET-1, $$$$p < 0.0001 v/s ET-1 + HAPL200, ###p < 0.001 v/s ET-1 + HAPL400). However, catalase activity was not improved at both doses of HAPL treatment

(Fig. 5C).

4. Discussion

Ischemic stroke is one of the leading causes of death and disability, where available therapeutic strategies mainly target the blood coagulation system (Bansal et al., 2013; Ghobrial et al., 2014; Marder et al., 2010) and not the neuronal cells effected due to ischemic injury. Tissue around the ischemic core, the ischemic penumbra is viable several hours after the stroke, where providing neuroprotective therapy at this juncture appears crucial in restoring the structure and function (Dirnagl et al., 1999; Ghobrial et al., 2014; Heiss, 2012). Increase in our understanding about the mechanisms for neuronal injury and the discovery of phytoconstituents from alternative medicine that target these mechanisms provide hope for disease modifying therapeutic strategies (Dirnagl et al., 1999; Sachdev et al., 2007). Here, we have identified hydroalcoholic extract of *Pluchea lanceolata*, an Ayurvedic medicinal plant to ameliorate ischemic hippocampal injury induced learning and memory deficits through its antioxidant properties.

The middle cerebral artery occlusion (MCAO) either by ligation or vasoconstriction using ET-1 is the most commonly used rodent model of ischemic hippocampal stroke (Yan et al., 2014). However, to achieve focal ischemic injury, we employed direct injection of ET-1 to the hippocampus which also brings functional deficit (Driscoll et al., 2008; Tsenov et al., 2007). Reproducibility and mortality rates are the concerns in MCAO that are taken care in direct injection of ET-1 (Sheng et al., 2015; Soleman et al., 2010). Similar methodology has been used to induce focal cerebral ischemia in the rat cerebral cortex (Nguemeni et al., 2015; Rakai and Antle, 2013) striatum (Abeysinghe et al., 2014; Fuxe et al., 1997) and amygdala (Sheng et al., 2015). This model of focal ischemic stroke has also been recently reproduced in non-human primates (Dai et al., 2017). Direct ET-1 infusion induced hippocampal injury led to learning and memory deficits in que-place water task (Driscoll et al., 2008). Severe cognitive disability was also noted in open field test, novel object recognition tasks (Sheng et al., 2015) and in Morris water maze (Faraji et al., 2014). Our observations are in concurrence with these studies, where cognitive skills in Morris water maze were significantly effected in ET-1 groups. Along with learning and memory function, hippocampus also play an important role in exploratory behaviour, especially in rearing (Johnson et al., 2012; Lever et al., 2006; Tanaka et al., 2012) and also in modulation of locomotion through its dopaminergic circuitry (Kempadoo et al., 2016; McNamara and Dupret, 2017). It was also evident in our study where open field exploratory behaviour was hampered along with increased anxiety as noted by number of fecal pellets expelled, and a considerable decrease in overall locomotion. Thus, direct intrahippocampal ET-1 injections evidently replicated overall functional dysfunction of hippocampal stroke.

Various neuromodulatory potentials of *P. lanceolata* plant extract were reported (Mundugaru et al., 2017; Srivastava et al., 2014; Srivastava and Shanker, 2012). The present work is first of its kind to reveal its efficacy in alleviating ischemic injury induced learning and memory deficits. The ability of HAPL to almost completely alleviate ischemia induced cognitive dysfunction in water maze test even at lower dose indicate its superior neuroprotective efficacy to maintain the primary function of hippocampus. Recovery from deficits in locomotion required higher HAPL dosage; solicit the differential efficacy of the plant extract on different pathways that were effected due to ET-1 mediated hippocampal stroke. Similar differential efficacy was noted within the sub-tests of open field behaviour evaluation. Number of squares crossed in the open field that tests the exploratory behaviour (Gould et al., 2001; Seibenhener and Wooten, 2015), which is mainly attributed to CA3 region of hippocampus (Mizuseki et al., 2012) was recovered almost to normal after HAPL treatment. Recovery was also noted in reducing anxiety levels as evaluated by fecal pellets expelled where dentate gyrus and CA1 are involved (Jimenez et al., 2018; Kheirbek et al., 2013). There was trend towards recovery in rearing behaviour at higher dose, whereas significance was achieved only in grooming behaviour. Thus, though it appeared to have lesser efficiency or required in higher concentrations to rescue few functions, *P. lanceolata* significantly rescued overall cognitive behaviour in ischemic hippocampal stroke indicating its neuroprotective potentials.

Loss of neuronal cells and the neurodegenerative phenotype of shrunken hyperdensed soma with pyknotic nucleus noted in the CA1 and CA3 hippocampal regions following ET-1 induced hippocampal ischemia were in agreement with earlier observations (Driscoll et al., 2008; Tsenov et al., 2007). Preserved cell number along with neuronal phenotype noted after *P. lanceolata* treatment provide histological basis for the preservation of cognitive behaviour. Interestingly, the rescue in the CA1 area was relatively more efficient compared to CA3, which was also noted in terms of differential behavioural recovery. CA1 is the most vulnerable region for ischemic injury, both in animal models (Farkas et al., 2007) and in stroke patients (Zola-Morgan et al., 1986). Ability of *P. lanceolata* to efficiently rescue the pyramidal cells from this area is thus promising and further studies are warranted to evaluate the active compounds in the extract and their molecular targets in CA1 hippocampal neurons.

Golgi staining is the first and still widely used method to evaluate the details of neuronal dendritic arborization (Narayanan et al., 2014). Though there are detailed histopathological studies conducted on ET-1 induced focal ischemic hippocampal injury, no understanding at the dendritic level is available. Dendritic spines and branches are the first site of degeneration in ischemic injury (Brown et al., 2008). The stunted length of both apical and basal dendrites and evident fall in the number of dendritic branches in CA1 and CA3 neurons noted in our study are in concurrence with studies on MCAO induced hippocampal stroke (Gillani et al., 2010); further validates ET-1 induced focal hippocampal stroke model. Our observation also reveals that the basal dendrites of CA3 neurons were least effected by ET-1 injection, whereas both basal and apical dendrites were severely effected in CA1 region. This is in agreement with other studies that indicate CA1 as the most vulnerable for ischemic injury (Farkas et al., 2007; Kirino, 1982; Pulsinelli et al., 1982; Zola-Morgan et al., 1986). The *P. lanceolata* treatment was affective in preserving the dendritic branching in both CA1 and CA3 hippocampal neurons in ischemic injury. Unlike what we noted with cresyl violet staining, only higher dose HAPL could salvage the branching points. It is interesting to note that, in ischemic group, the high dose treatment with HAPL significantly increased dendritic intersections more than the control. Similar observations were reported earlier with choline and DHA supplementation in normal rats (Holguin et al., 2008; Wurtman, 2008). This indicates that *P. lanceolata* extract might contain important tropic factors, antioxidants, *etc.*, and prophylactic treatment of the same might have a better outcome. Further studies may be conducted to understand whether the plant extract can be used as dietary supplement to boost learning and memory function even in healthy individuals.

Severe oxidative stress and lipid peroxidation play key role in ischemic brain injury induced neuronal death (Nakashima et al., 1999). ET-1 induced ischemia, especially during reperfusion injury has been shown to increase reactive oxygen species (ROS) level, subsequently leading to inflammation causing secondary ischemic damage (Driscoll et al., 2008; Wang et al., 2007). We noted similar increase in hippocampal lipid peroxidation and reduction in antioxidant enzymes such as catalase and glutathione peroxidase in ET-1 group. The ability of *P. lanceolata to bring the glutathione peroxidase levels to normal solicit its potential to increase antioxidants level to protect the hippocampal neurons, which was earlier noted in peripheral tissues* (Jahangir and Sultana, 2006). This in-turn significantly attenuated ischemia induced lipid peroxidation after HAPL treatment. Interestingly, we noted that the antioxidant property of *P. lanceolata is exerted through glutathione peroxidase and not catalase. It indicates that the glutathione peroxidase may be one of the priority targets to achieve functional and histological recovery in ischemic*

injury, and P. lanceolata exert its neuroprotection through this enzyme. Further studies are warranted to confirm these findings. Taraxasterol and its naturally occurring acetate derivatives from *P. lanceolata* are known to protect lipopolysaccharide induced neuroinflammation by downregulating the TNF-α, IFN-γ, and IL-6 (Srivastava et al., 2014). Thus, hippocampal neuroprotection noted after *P. lanceolata* treatment may also be attributed to its anti-inflammatory properties (Chen et al., 2011). Its acetyl cholinesterase inhibitory actions to maintain acetyl choline levels (Srivastava and Shanker, 2012) might also have played role in preserving cognitive abilities in ischemic conditions.

5. Conclusion

Ischemic brain injury existed before its description in modern medicine, so does the treatment strategies in the traditional system, mainly using phytoconstituents. Understanding the mechanisms through which neuroprotective function is being executed by these medicinal plants in modern medicine perspective may provide an immediate, reliable alternative mode of disease modifying treatment (Lakhotia, 2013). In this regard, we provide first evidence for wide spectrum neuroprotective properties of *P. lanceolata* treatment in a disease model of ischemic hippocampal injury. Rats with ischemia when treated with *P. lanceolata* revealed evident preservation of cognitive functions, along with maintenance of pyramidal neurons in both CA1 and CA3 sub-regions, with intact dendritic architecture. There are differences in the CA1 and CA3 sub-regions regarding the projections and intrinsic circuits. CA3 possess strong recurrent collateral system whereas CA1 neurons are organized largely in parallel (Amaral and Lavenex, 2007; Amaral and Witter, 1989), performing distinct computations to carry out specific functions (Jimenez et al., 2018; Mizuseki et al., 2012). This was also evident in our study where *P. lanceolata* revealed differential efficacy in preserving the CA1 and CA3 neurons and their behavioural correlates, which was also dose depended. Its ability to protect most vulnerable CA1 neurons with superior efficiency through its antioxidant properties make it a potential alternative disease modifying treatment for ischemic hippocampal stroke. It is necessary to further evaluate whether the *P. lanceolata* has similar beneficial effect in other brain regions and in global ischemic conditions.

Funding

This work was a part of the extramural research funding by Ministry of AYUSH, Govt. of India to Ravi Mundugaru (Z.28015/209/2015-HPC-EMR). We also acknowledge the intramural funds and laboratory facilities extended by SDM Centre for Research in Ayurveda and Allied Sciences, Udupi, India.

Conflict of interest statement

The authors declare that the research was conducted in the absence of any commercial or financial relationships that could be construed as a potential conflict of interest.

Ethics statement

All applicable international, national, and/or institutional guidelines for the care and use of animals were followed. All procedures performed in studies involving animals were in accordance with the ethical standards of the institution or practice at which the studies were conducted.

References

Abeysinghe, H.C., Bokhari, L., Dusting, G.J., Roulston, C.L., 2014. Brain remodelling following endothelin-1 induced stroke in conscious rats. PLoS One 9, e97007.
Amaral, D.G., Witter, M.P., 1989. The three-dimensional organization of the hippocampal formation: a review of anatomical data. Neuroscience 31, 571–591.
Amaral, D., Lavenex, P., 2007. Hippocampal Neuroanatomy. Oxford University Press, New York, NY.
Baba, A., 1998. Role of endothelin B receptor signals in reactive astrocytes. Life Sci. 62, 1711–1715.
Bansal, S., Sangha, K.S., Khatri, P., 2013. Drug treatment of acute ischemic stroke. Am. J. Cardiovasc. Drugs 13, 57–69.
Bansinath, M., Bose, A.C., Hema, S., Guruswami, M.N., 1982. Interaction of metamizol with some hypnotics in rats. Arch. Int. Pharmacodyn. Ther. 260, 14–27.
Bhagwat, D.P., Kharya, M.D., Bani, S., Kaul, A., Kour, K., Chauhan, P.S., Suri, K.A., Satti, N.K., 2010. Immunosuppressive properties of Pluchea lanceolata leaves. Indian J. Pharmacol. 42, 21–26.
Bhattacharya, S.K., Satyan, K.S., Chakrabarti, A., 1997. Anxiogenic action of caffeine: an experimental study in rats. J. Psychopharmacol. 11, 219–224.
Blomstrand, F., Venance, L., Siren, A.L., Ezan, P., Hanse, E., Glowinski, J., Ehrenreich, H., Giaume, C., 2004. Endothelins regulate astrocyte gap junctions in rat hippocampal slices. Eur. J. Neurosci. 19, 1005–1015.
Bromley-Brits, K., Deng, Y., Song, W., 2011. Morris water maze test for learning and memory deficits in Alzheimer's disease model mice. J. Vis. Exp.
Brown, C.E., Wong, C., Murphy, T.H., 2008. Rapid morphologic plasticity of peri-infarct dendritic spines after focal ischemic stroke. Stroke 39, 1286–1291.
Chen, H., Yoshioka, H., Kim, G.S., Jung, J.E., Okami, N., Sakata, H., Maier, C.M., Narasimhan, P., Goeders, C.E., Chan, P.H., 2011. Oxidative stress in ischemic brain damage: mechanisms of cell death and potential molecular targets for neuroprotection. Antioxid. Redox Signal. 14, 1505–1517.
Dai, P., Huang, H., Zhang, L., He, J., Zhao, X., Yang, F., Zhao, N., Yang, J., Ge, L., Lin, Y., Yu, H., Wang, J., 2017. A pilot study on transient ischemic stroke induced with endothelin-1 in the rhesus monkeys. Sci. Rep. 7, 45097.
Dalley, J.W., Cardinal, R.N., Robbins, T.W., 2004. Prefrontal executive and cognitive functions in rodents: neural and neurochemical substrates. Neurosci. Biobehav. Rev. 28, 771–784.
Dirnagl, U., Iadecola, C., Moskowitz, M.A., 1999. Pathobiology of ischaemic stroke: an integrated view. Trends Neurosci. 22, 391–397.
Donnan, G.A., Fisher, M., Macleod, M., Davis, S.M., 2008. Stroke. Lancet 371, 1612–1623.
Driscoll, I., Hong, N.S., Craig, L.A., Sutherland, R.J., McDonald, R.J., 2008. Enhanced cell death and learning deficits after a mini-stroke in aged hippocampus. Neurobiol. Aging 29, 1847–1858.
Faraji, J., Soltanpour, N., Moeeini, R., Roudaki, S., Soltanpour, N., Abdollahi, A.A., Metz, G.A., 2014. Topographical disorientation after ischemic mini infarct in the dorsal hippocampus: whispers in silence. Front. Behav. Neurosci. 8, 261.
Farkas, E., Luiten, P.G., Bari, F., 2007. Permanent, bilateral common carotid artery occlusion in the rat: a model for chronic cerebral hypoperfusion-related neurodegenerative diseases. Brain Res. Rev. 54, 162–180.
Fuxe, K., Bjelke, B., Andbjer, B., Grahn, H., Rimondini, R., Agnati, L.F., 1997. Endothelin-1 induced lesions of the frontoparietal cortex of the rat. A possible model of focal cortical ischemia. Neuroreport 8, 2623–2629.
Ghobrial, G.M., Chalouhi, N., Zohra, M., Dalyai, R.T., Ghobrial, M.L., Rincon, F., Flanders, A.E., Tjoumakaris, S.I., Jabbour, P., Rosenwasser, R.H., Fernando Gonzalez, L., 2014. Saving the ischemic penumbra: endovascular thrombolysis versus medical treatment. J. Clin. Neurosci. 21, 2092–2095.
Gillani, R.L., Tsai, S.Y., Wallace, D.G., O'Brien, T.E., Arhebamen, E., Tole, M., Schwab, M.E., Kartje, G.L., 2010. Cognitive recovery in the aged rat after stroke and anti-Nogo-A immunotherapy. Behav. Brain Res. 208, 415–424.
Gopalakrishanan, S., Babu, M.R., Thangarajan, R., Punja, D., Jaganath, V.D., Kanth, A.B., Rao, M., Rai, K.S., 2016. Impact of seasonal variant temperatures and laboratory room ambient temperature on mortality of rats with ischemic brain injury. J. Clin. Diagn. Res. 10, Cf01–5.
Gould, T.J., Keith, R.A., Bhat, R.V., 2001. Differential sensitivity to lithium's reversal of amphetamine-induced open-field activity in two inbred strains of mice. Behav. Brain Res. 118, 95–105.
Heiss, W.D., 2012. The ischemic penumbra: how does tissue injury evolve? Ann. N. Y. Acad. Sci. 1268, 26–34.
Holguin, S., Martinez, J., Chow, C., Wurtman, R., 2008. Dietary uridine enhances the improvement in learning and memory produced by administering DHA to gerbils. FASEB J. 22, 3938–3946.
Hughes, P.M., Anthony, D.C., Ruddin, M., Botham, M.S., Rankine, E.L., Sablone, M., Baumann, D., Mir, A.K., Perry, V.H., 2003. Focal lesions in the rat central nervous system induced by endothelin-1. J. Neuropathol. Exp. Neurol. 62, 1276–1286.
Hynynen, M.M., Khalil, R.A., 2006. The vascular endothelin system in hypertension–recent patents and discoveries. Recent Pat. Cardiovasc. Drug Discov. 1, 95–108.
Iadecola, C., Alexander, M., 2001. Cerebral ischemia and inflammation. Curr. Opin. Neurol. 14, 89–94.
Jahangir, T., Sultana, S., 2006. Modulatory effects of Pluchea lanceolata against chemically induced oxidative damage, hyperproliferation and two-stage renal carcinogenesis in Wistar rats. Mol. Cell. Biochem. 291, 175–185.
Jahangir, T., Khan, T.H., Prasad, L., Sultana, S., 2005. Pluchea lanceolata attenuates cadmium chloride induced oxidative stress and genotoxicity in Swiss albino mice. J. Pharm. Pharmacol. 57, 1199–1204.
Jimenez, J.C., Su, K., Goldberg, A.R., Luna, V.M., Biane, J.S., Ordek, G., Zhou, P., Ong, S.K., Wright, M.A., Zweifel, L., Paninski, L., Hen, R., Kheirbek, M.A., 2018. Anxiety cells in a hippocampal-hypothalamic circuit. Neuron 97, 670–683 e6.
Johnson, A., Varberg, Z., Benhardus, J., Maahs, A., Schrater, P., 2012. The hippocampus and exploration: dynamically evolving behavior and neural representations. Front. Hum. Neurosci. 6, 216.
Jyothi, H.J., Vidyadhara, D.J., Mahadevan, A., Philip, M., Parmar, S.K., Manohari, S.G., Shankar, S.K., Raju, T.R., Alladi, P.A., 2015. Aging causes morphological alterations

in astrocytes and microglia in human substantia nigra pars compacta. Neurobiol. Aging 36, 3321–3333.
Kempadoo, K.A., Mosharov, E.V., Choi, S.J., Sulzer, D., Kandel, E.R., 2016. Dopamine release from the locus coeruleus to the dorsal hippocampus promotes spatial learning and memory. Proc. Natl. Acad. Sci. U. S. A. 113, 14835–14840.
Kheirbek, M.A., Drew, L.J., Burghardt, N.S., Costantini, D.O., Tannenholz, L., Ahmari, S.E., Zeng, H., Fenton, A.A., Hen, R., 2013. Differential control of learning and anxiety along the dorsoventral axis of the dentate gyrus. Neuron 77, 955–968.
Kirino, T., 1982. Delayed neuronal death in the gerbil hippocampus following ischemia. Brain Res. 239, 57–69.
Lakhotia, S.C., 2013. Neurodegeneration disorders need holistic care and treatment - can ayurveda meet the challenge? Ann. Neurosci. 20, 1–2.
Langdon, K.D., Maclellan, C.L., Corbett, D., 2010. Prolonged, 24-h delayed peripheral inflammation increases short- and long-term functional impairment and histopathological damage after focal ischemia in the rat. J. Cereb. Blood Flow Metab. 30, 1450–1459.
Lever, C., Burton, S., O'Keefe, J., 2006. Rearing on hind legs, environmental novelty, and the hippocampal formation. Rev. Neurosci. 17, 111–133.
Marder, V.J., Jahan, R., Gruber, T., Goyal, A., Arora, V., 2010. Thrombolysis with plasmin: implications for stroke treatment. Stroke 41, S45–9.
McNamara, C.G., Dupret, D., 2017. Two sources of dopamine for the hippocampus. Trends Neurosci. 40, 383–384.
Mizuseki, K., Royer, S., Diba, K., Buzsaki, G., 2012. Activity dynamics and behavioral correlates of CA3 and CA1 hippocampal pyramidal neurons. Hippocampus 22, 1659–1680.
Mohanty, S., Srivastava, P., Maurya, A.K., Cheema, H.S., Shanker, K., Dhawan, S., Darokar, M.P., Bawankule, D.U., 2013. Antimalarial and safety evaluation of Pluchea lanceolata (DC.) Oliv. & Hiern: in-vitro and in-vivo study. J. Ethnopharmacol. 149, 797–802.
Muir, K.W., Tyrrell, P., Sattar, N., Warburton, E., 2007. Inflammation and ischaemic stroke. Curr. Opin. Neurol. 20, 334–342.
Mundugaru, R., Sivanesan, S., Udaykumar, P., Rao, N., Chandra, N., 2017. Protective effect of Pluchea lanceolata against aluminum chloride-induced neurotoxicity in Swiss albino mice. Pharmacogn. Mag. 13, S567–S572.
Nakashima, M., Niwa, M., Iwai, T., Uematsu, T., 1999. Involvement of free radicals in cerebral vascular reperfusion injury evaluated in a transient focal cerebral ischemia model of rat. Free Radic. Biol. Med. 26, 722–729.
Narayanan, S.N., Jetti, R., Gorantla, V.R., Kumar, R.S., Nayak, S., Bhat, P.G., 2014. Appraisal of the effect of brain impregnation duration on neuronal staining and morphology in a modified Golgi-Cox method. J. Neurosci. Methods 235, 193–207.
Nguemeni, C., Gomez-Smith, M., Jeffers, M.S., Schuch, C.P., Corbett, D., 2015. Time course of neuronal death following endothelin-1 induced focal ischemia in rats. J. Neurosci. Methods 242, 72–76.
Ohkawa, H., Ohishi, N., Yagi, K., 1979. Assay for lipid peroxides in animal tissues by thiobarbituric acid reaction. Anal. Biochem. 95, 351–358.
Prasad, D.N., Gode, K.D., Sinha, P.S., Das, P.K., 1965. Preliminary phytochemical and pharmacological studies on Plutchea lanceolata, Linn. Indian J. Med. Res. 53, 1062–1068.
Pulsinelli, W.A., Brierley, J.B., Plum, F., 1982. Temporal profile of neuronal damage in a model of transient forebrain ischemia. Ann. Neurol. 11, 491–498.
Rakai, B.D., Antle, M.C., 2013. Lesion size and behavioral deficits after endothelin-1-induced ischemia are not dependent on time of day. J. Stroke Cerebrovasc. Dis. 22, 397–405.
Rotruck, J.T., Pope, A.L., Ganther, H.E., Swanson, A.B., Hafeman, D.G., Hoekstra, W.G., 1973. Selenium: biochemical role as a component of glutathione peroxidase. Science 179, 588–590.
Rozyczka, J., Figiel, M., Engele, J., 2004. Endothelins negatively regulate glial glutamate transporter expression. Brain Pathol. 14, 406–414.
Sachdev, P.S., Chen, X., Joscelyne, A., Wen, W., Altendorf, A., Brodaty, H., 2007. Hippocampal size and dementia in stroke patients: the Sydney stroke study. J. Neurol. Sci. 260, 71–77.
Seibenhener, M.L., Wooten, M.C., 2015. Use of the open field maze to measure locomotor and anxiety-like behavior in mice. J. Vis. Exp. e52434.
Sharma, P.V., 2005. Dravyaguna Vigyan. Chaukhambha Bharti Academy, Varanasi, India.
Sheng, T., Zhang, X., Wang, S., Zhang, J., Lu, W., Dai, Y., 2015. Endothelin-1-induced mini-stroke in the dorsal hippocampus or lateral amygdala results in deficits in learning and memory. J. Biomed. Res. 29, 362–369.
Sholl, D.A., 1953. Dendritic organization in the neurons of the visual and motor cortices of the cat. J. Anat. 87, 387–406.
Sinha, A.K., 1972. Colorimetric assay of catalase. Anal. Biochem. 47, 389–394.
Soleman, S., Yip, P., Leasure, J.L., Moon, L., 2010. Sustained sensorimotor impairments after endothelin-1 induced focal cerebral ischemia (stroke) in aged rats. Exp. Neurol. 222, 13–24.
Srivastava, P., Shanker, K., 2012. Pluchea lanceolata (Rasana): chemical and biological potential of Rasayana herb used in traditional system of medicine. Fitoterapia 83, 1371–1385.
Srivastava, P., Mohanti, S., Bawankule, D.U., Khan, F., Shanker, K., 2014. Effect of Pluchea lanceolata bioactives in LPS-induced neuroinflammation in C6 rat glial cells. Naunyn Schmiedebergs Arch. Pharmacol. 387, 119–127.
Suresh, S.N., Chavalmane, A.K., Dj, V., Yarreiphang, H., Rai, S., Paul, A., Clement, J.P., Alladi, P.A., Manjithaya, R., 2017. A novel autophagy modulator 6-Bio ameliorates SNCA/alpha-synuclein toxicity. Autophagy 13, 1221–1234.
Tanaka, S., Young, J.W., Halberstadt, A.L., Masten, V.L., Geyer, M.A., 2012. Four factors underlying mouse behavior in an open field. Behav. Brain Res. 233, 55–61.
Tsenov, G., Mateffyova, A., Mares, P., Otahal, J., Kubova, H., 2007. Intrahippocampal injection of endothelin-1: a new model of ischemia-induced seizures in immature rats. Epilepsia 48 (Suppl. 5), 7–13.
Vidyadhara, D.J., Yarreiphang, H., Abhilash, P.L., Raju, T.R., Alladi, P.A., 2016. Differential expression of calbindin in nigral dopaminergic neurons in two mice strains with differential susceptibility to 1-methyl-4-phenyl-1,2,3,6-tetrahydropyridine. J. Chem. Neuroanat. 76, 82–89.
Vidyadhara, D.J., Yarreiphang, H., Raju, T.R., Alladi, P.A., 2017. Admixing of MPTP-resistant and susceptible mice strains augments nigrostriatal neuronal correlates to resist MPTP-induced neurodegeneration. Mol. Neurobiol. 54, 6148–6162.
Vorhees, C.V., Williams, M.T., 2006. Morris water maze: procedures for assessing spatial and related forms of learning and memory. Nat. Protoc. 1, 848–858.
Wang, Q., Tang, X.N., Yenari, M.A., 2007. The inflammatory response in stroke. J. Neuroimmunol. 184, 53–68.
Wurtman, R.J., 2008. Synapse formation and cognitive brain development: effect of docosahexaenoic acid and other dietary constituents. Metabolism 57 (Suppl. 2), S6–10.
Yan, H., Mitschelen, M., Toth, P., Ashpole, N.M., Farley, J.A., Hodges, E.L., Warrington, J.P., Han, S., Fung, K.M., Csiszar, A., Ungvari, Z., Sonntag, W.E., 2014. Endothelin-1-induced focal cerebral ischemia in the growth hormone/IGF-1 deficient Lewis Dwarf rat. J. Gerontol. A: Biol. Sci. Med. Sci. 69, 1353–1362.
Zola-Morgan, S., Squire, L.R., Amaral, D.G., 1986. Human amnesia and the medial temporal region: enduring memory impairment following a bilateral lesion limited to field CA1 of the hippocampus. J. Neurosci. 6, 2950–2967.